DOI: 10.18721/JCSTCS.14206
УДК 531.383

MICROMECHANICAL SENSORS DESIGN METHOD BASED ON SYSTEM-LEVEL MODELING

A.T. Tulaev, A.V. Styazhkina, A.S. Kozlov, Ya.V. Belyaev

Concern CSRI Elektropribor, JSC,
St. Petersburg, Russian Federation

This paper proposes a design method for micromechanical inertial sensors with force feedback electromechanical loop with delta-sigma modulator. Development of such sensors requires application of modern design methods, including modeling at system level, model refinement based on results of finite element modeling and modeling of individual electronic blocks at circuit level, as well as implementation of a digital twin based on results of an experimental study of sensors samples. Such a complex approach to sensor design is caused by high requirements to sensor characteristics (both in terms of dynamic range and accuracy), the need to consider the impact of external factors and the various physics to describe the processes, the impossibility of rapid prototyping, the influence of technological process parameters on sensor characteristics, etc. In this regard, this paper proposes a comprehensive method for the design of micromechanical sensors based on the construction of the system model. This paper represents the results of an experimental study of the force feedback type sensor using the proposed method.

Keywords: micromechanical sensor, MEMS, delta-sigma modulator, system level model, digital twin.

Citation: Tulaev A.T., Styazhkina A.V., Kozlov A.S., Belyaev Ya.V. Micromechanical sensors design method based on system-level modeling. Computing, Telecommunications and Control, 2021, Vol. 14, No. 2, Pp. 79–92. DOI: 10.18721/JCST-CS.14206

МЕТОДИКА ПРОЕКТИРОВАНИЯ МИКРОМЕХАНИЧЕСКОГО ДАТЧИКА НА ОСНОВЕ КОМПЛЕКСНОЙ СИСТЕМНОЙ МОДЕЛИ

А.Т. Тулаев, А.В. Стяжкина, А.С. Козлов, Я.В. Беляев

ЦНИИ «Электроприбор»,
Санкт-Петербург, Российская Федерация

Предложена методика проектирования микромеханических инерциальных датчиков компенсационного типа, в контуре управления которых применен дельта-сигма модулятор. Разработка таких датчиков требует современных методов проектирования, включающих моделирование на системном уровне, уточнение модели по результатам конечно-элементного моделирования и моделирования отдельных блоков контура управления на схемотехническом уровне, а также реализацию цифрового двойника по результатам экспериментального исследования образцов. Такой комплексный подход к проектированию обусловлен высокими требованиями к характеристикам датчика (как в части динамического диапазона, так и в части точностных характеристик), необходимостью учета различных физик для описания процессов, необходимостью оценки влияния внешних воздействующих факторов, невозможностью проведения быстрого макетирования, необходимостью учета влияния на характеристики датчика параметров технологического процесса и др. В связи с этим в статье предложена комплексная методика проектирования микромеханических датчиков на основе системной модели. Приведены результаты экспериментального исследования датчика компенсационного типа с применением предложенной методики.

Ключевые слова: микромеханический датчик, МЭМС, дельта-сигма модулятор, системная модель, цифровой двойник.

Ссылка при цитировании: Tulaev A.T., Styazhkina A.V., Kozlov A.S., Belyaev Ya.V. Micromechanical sensors design method based on system-level modeling // Computing, Telecommunications and Control. 2021. Vol. 14. No. 2. Pp. 79–92. DOI: 10.18721/JCSTCS.14206

Introduction

Due to their small size and power consumption, as well as their low cost in mass production, microelectromechanical sensors (MEMS) are an integral part of modern small-size navigation and motion control systems [1, 2]. Inertial MEMS include micromechanical accelerometers (MMA) and gyroscopes (MMG), designed to determine the linear acceleration and angular velocity of the object, respectively. The use in navigation and motion control systems imposes strict requirements on MMAs and MMGs [1, 2]:

- wide measurement range from ± 200 to ± 7000°/s – for MMG and from ± 2 to ± 50g – for MMA;
- low non-linearity of the sensor output – at level of 0.01 %;
- wide dynamic range – more than 100 dB;
- high temporal stability of output signal – at 5°/h for MMG and 0.01 mg for MMA
- robustness to external influences (temperature variations from minus 60 to plus 85°C, impact and vibration, etc.) – at 100°/h for MMG and 1 mg for MMA.

Such requirements can be achieved by applying comprehensive solutions at the design level:

- by using multiple proof mass sensing elements [3–6];
- by utilizing specialized integrated circuits, in particular compensation circuits with a delta-sigma modulator in the control loop [7–17];
- by using temperature stabilization systems, etc.

Complication of inertial MEMS architecture, impossibility of fast prototyping, necessity of simultaneous modelling of blocks of integrated circuit and sensing element, the need to consider influence of external influencing factors and different physics for describing processes, as well as influence of technological process parameters require to design MEMS based on an accurate mathematical model. The existing design methodologies and mathematical models of inertial MEMS they are based on [18, 19] have a number of drawbacks:

- the electronic blocks processing output signal are not considered at all or considered in a simplified manner;
- the sensing element is represented by lumped parameters (elastic rigid suspension stiffness, electrode structure capacitance), determined separately analytically or by finite element analysis;
- the model does not take into account experimental data.

In this regard, this paper proposes a comprehensive methodology for designing capacitive inertial MEMS based on the system model that takes into account the main electronic blocks of output signal processing, the results of coupled finite-element modelling of the sensing element and the results of experimental studies. Thus, a prototype of a digital twin sensor is implemented in the course of the design, which allows increasing its accuracy. The methodology is considered on the example of MMA and MMG developed by CSRI Elektropribor, JSC.

Object of study

The main parts of capacitive MMA and MMG are:

- a sensing element (SE), designed to convert the input acceleration into a change in capacitance;

- application-specific integrated circuit (ASIC) designed to convert the capacitance change into digital data and control the SE in case of the compensation operating mode of sensor.

The SE can be described by second order transfer function based on system of equations:

$$J\begin{bmatrix}\ddot{\alpha}\\ \ddot{\beta}\\ \ddot{\gamma}\end{bmatrix}+D\begin{bmatrix}\dot{\alpha}\\ \dot{\beta}\\ \dot{\gamma}\end{bmatrix}+K\begin{bmatrix}\alpha\\ \beta\\ \gamma\end{bmatrix}=M,$$
$$m\begin{bmatrix}\ddot{x}\\ \ddot{y}\\ \ddot{z}\end{bmatrix}+d\begin{bmatrix}\dot{x}\\ \dot{y}\\ \dot{z}\end{bmatrix}+k\begin{bmatrix}x\\ y\\ z\end{bmatrix}=F, \quad (1)$$

where x, y and z – displacement of proof mass along the axes OX, OY, OZ respectively; α, β, γ – rotation angles of proof mass around the axes OX, OY, OZ respectively; J – inertia matrix; m – proof mass; d and D – linear and angular damping matrices; k and K – linear and angular stiffness matrix; F and M – matrix of forces and moments, acting on the proof mass.

For the case of translational motion of the proof mass along one axis, in the absence of electrical and mechanical connections along the other axes, system (1) can be transformed into the following form:

$$m\ddot{x}+d_x\dot{x}+k_x x=F_x, \quad (2)$$

where d_y – damping factor along the axis OY; k_y – stiffness along the axis OY; F_y – the projection of the acting forces on the axis OY.

In order to convert the proof mass displacement into a change in capacitance and to create the electrostatic force that provides the compensation mode SE includes an electrode structure characterized by a capacitance-displacement relationship $C(x)$ and electrostatic force from electrode voltage relationship $F(x, U)$.

The further conversion of capacitance to voltage is done in the IC. In order to achieve low noise, wide dynamic range and low non-linearity [7], an electronic feedback control loop based on digital delta-sigma modulator that forms an electromechanical loop with SE is implemented. Together with the implementation of time division multiplexing of sensing and driving signals, this reduces the influence of undesirable nonlinear mechanical effects, nonlinearities in the capacitive electrode structure, and the mechanical and electrical parasitic interactions caused by the use of silicon-on-insulator manufacture technology of the SE.

Ideally, equation (2) can be used to describe a uniaxial SE of MMA with the sensitivity axis directed along the OX axis.

The difference between MMG and MMA is that its principle of operation is based on conversion of vibrational energy of SE on the primary axis into vibrational energy orthogonal to it secondary axis. The oscillations along the secondary axis contain information about the measured angular velocity acting on the proof mass of the MMG along the sensitivity axis orthogonal to the first two axes.

In ideal case, the behavior of single axis RR-type MMG SE (Fig. 1) can be described by the following equation:

$$\begin{cases} J_\gamma\ddot{\gamma}+D_\gamma\dot{\gamma}+K_\gamma\gamma=M_{EL}, \\ J_\alpha\ddot{\alpha}+D_\alpha\dot{\alpha}+K_\alpha\alpha=M_K, \end{cases} \quad (3)$$

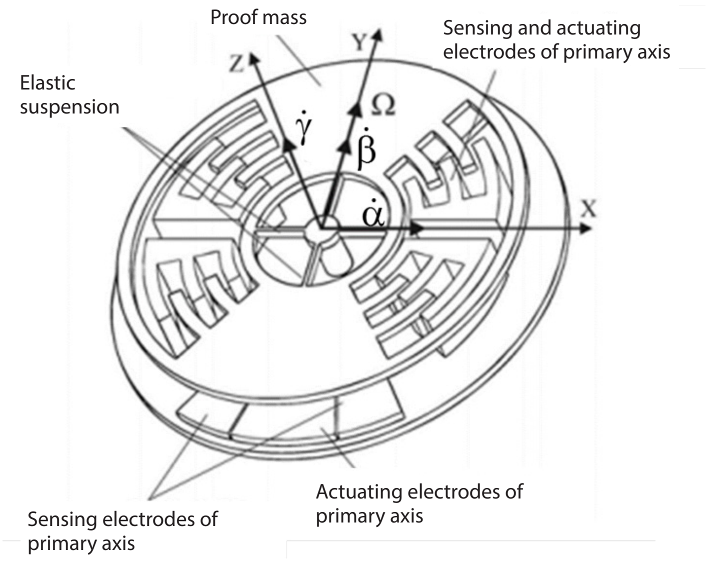

Fig. 1. Schematic diagram of MMG SE developed by CSRI Elektropribor, JSC

where γ, α – angular displacement of the proof mass along the primary and secondary axes respectively; D_γ, D_α – damping coefficients of the proof mass along the primary and secondary axes; K_γ, K_α – coefficients of angular stiffness along the primary and secondary axes; Ω_y – projection of angular velocity of SE to sensitivity axis; J_γ, J_α – moment of inertia of the proof mass relative to the primary and secondary axes; M_{EM} – electrostatic moment acting on the proof mass; $M_K = -2J_\alpha \Omega_y \dot{\gamma}$ – Coriolis moment.

Regarding this, the control system of the MMG working in the compensation mode, in addition to the circuit with secondary axis feedback, must have a circuit for excitation and stabilization of the primary oscillations. In this case, the accuracy of primary oscillation amplitude directly affects the accuracy of the sensor.

Design methodology of the inertial MEMS

The design methodology is shown in Fig. 2 in the form of block diagram.

The methodology is split into several steps. The first step is to build a linear system model of the force feedback sensor. The objectives of this stage are:

- estimate the initial parameters of the mechanical part of the SE, such as stiffness and damping coefficients;
- estimate the conversion coefficients of displacement into change in capacitance and of electrode voltage into electrostatic force, characterizing the electrode structure of the SE;
- parameter estimation of main integrated circuit (IC) blocks: capacitance-to-voltage converter (CVC), low-pass filter (LPF), analog-to-digital converter (ADC) and electronic blocks of delta-sigma modulator (ΣΔ-M).

In the second stage, the developed system model is refined taking into account the features of SE and IC, such as the type of electrode structure, parasitic electrostatic forces arising between the sensing electrodes, sensing and excitation method of SE, noise level of SE and IC [19]. This stage allows estimating the impact of the parameters due to a certain SE and IC architecture on the device behavior embedded in the linear model. In the third stage, the nonlinear behavioral system model is complemented by the results of finite element modelling of the SE [20] and schematic-level simulation of the output signal processing circuit [21]. At this stage, the parameters of the developed SE are verified and corrected: parameters of the elastic rigid suspension and electrode structure, as well as damping coefficient are specified, parasitic ca-

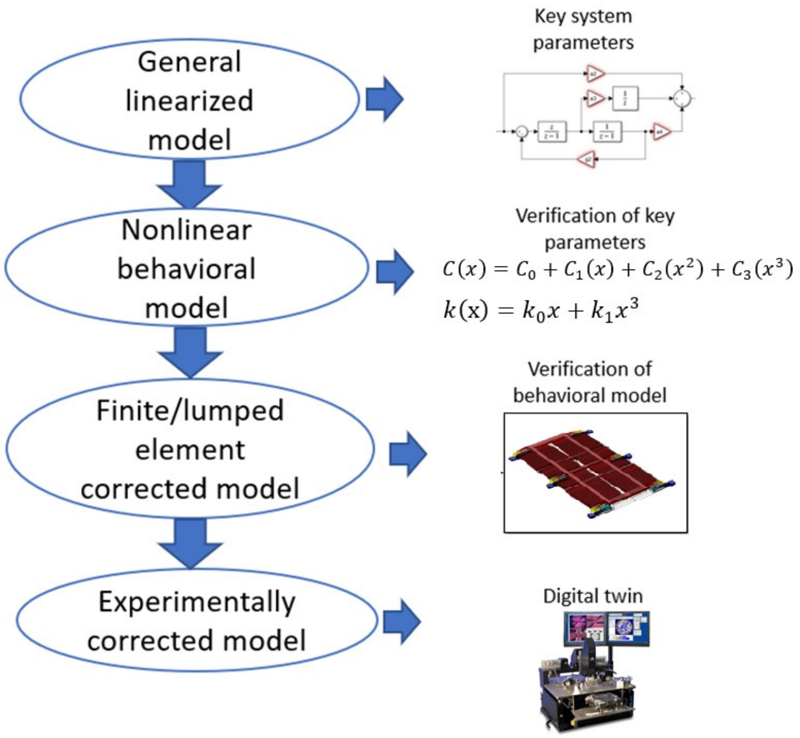

Fig. 2. Block diagram of design methodology

pacitances are added. In addition, the characteristics of the electronic blocks in the IC are specified based on the results of simulation for particular blocks.

In the final design stage, the model is further improved on the basis of experimentally obtained characteristics, such as temperature dependencies, thus implementing the digital twin concept.

General linearized system model

The control unit for a MMG with the characteristics given in the introduction must comply with the following requirements:

- form a time division multiplexing of sensing and driving signals;
- provide a defined level of non-linearity, due to the electrostatic force generated in the presence of voltage on the SE electrodes;
- provide the required dynamic range and noise level.

The requirements described above determine the design of the control unit based on a sigma-delta modulator (ΣΔ-M). Required dynamic range is achieved by oversampling and filtering that shifts quantization noise into the higher frequency band (Noise-shaping) [7]. So, the 4th order ΣΔ-M realizes dynamic range of more than 100dB.

The proof mass of the SE, captured by electrostatic feedback, allows the mechanical transfer function of the SE to act as a part of the ΣΔ-M and increases the order of the delta-sigma modulator by 2 without implementing additional integration units [7–15].

The possibility of designing an electromechanical ΣΔ-M emerges from the equivalence of the noise transfer functions of an all-electronic 4th order ΣΔ-M and an electromechanical ΣΔ-M formed by a SE and a 2nd order ΣΔ-M. Fig. 3 shows the output spectrum of a ΣΔ-M with identical noise transfer functions of an all-electronic and a 4th order electromechanical ΣΔ-M. The figure shows the equivalence of the spectrum of the electrical and electromechanical delta-sigma modulator output signals, which indicates that the electronic part of the electromechanical delta-sigma modulator is properly tuned to

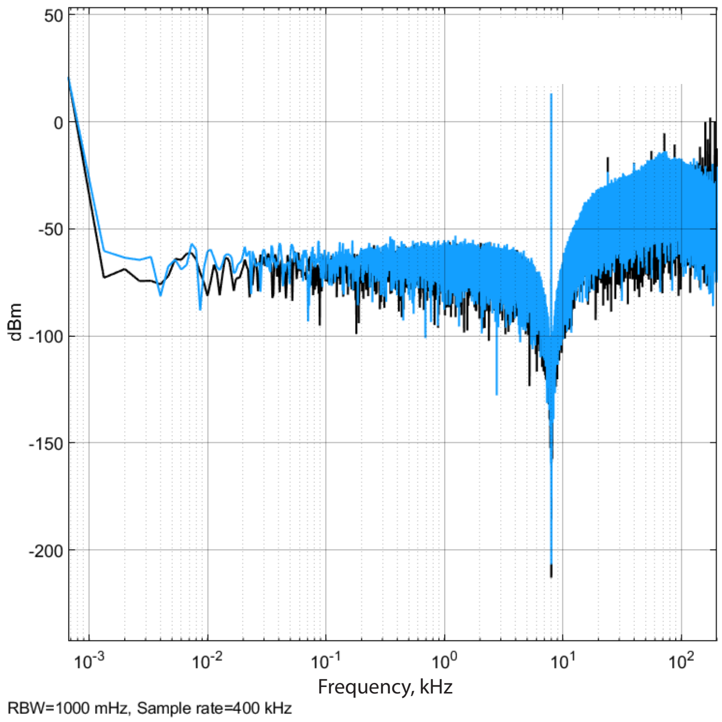

Fig. 3. Spectrum of the 4th order all-electronic and electromechanical ΣΔ-M
(–) – full electrical; (–) – electromechanical

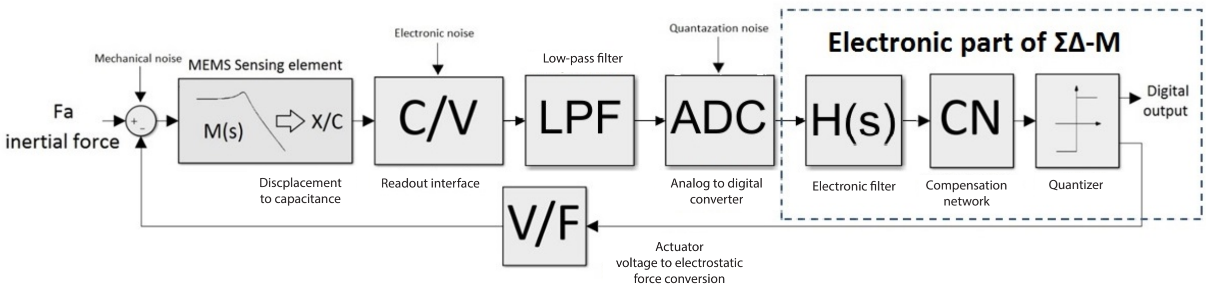

Fig. 4. Block diagram of the secondary oscillation loop

a certain eigenfrequency of the SE. Fig. 4 is obtained at a sampling rate of 400 kHz and a frequency resolution of 1 Hz.

In accordance with the methodology, a linear system model of the MMG was designed. The block diagram of the secondary oscillation loop is shown in Fig. 4.

The model consists of the following main elements:

1) Sensing element

The transfer functions formed by equation (3) are used to describe the SE. The values of stiffness and damping coefficients correspond to eigenfrequencies of primary and secondary oscillation modes of 8 and 8.2 kHz, respectively; quality factors are 80000 and 3000. Moments of inertia with respect to the primary and secondary axes are $6.77 \cdot 10^{-13}$ and $4.3 \cdot 10^{-13}$ kg·m^2.

Electrode structure of an RR-type SE is described by coefficients of conversion of angular displacement into change of capacitance and conversion of electrode voltage into torque. Values of coefficients for primary axis electrode structure are $7.2 \cdot 10^{-11}$ F/rad and $1.8 \cdot 10^{-11}$ $V^2 \cdot m/N$ and for secondary axis electrode structure are $1.98 \cdot 10^{-9}$ F/rad and $1.74 \cdot 10^{-10}$ $V^2 \cdot m/N$.

2) Capacitance-to-voltage converter

We chose a switched capacitor circuit CVC because it utilizes the following features:

- adjustment of the conversion coefficient by means of control registers;
- implementation of the required values of resistors and capacitors with limited area;
- use of bias compensation techniques to improve the parameters.

In addition, such circuit has a low sensitivity to temperature changes and a reduced noise level.

In accordance with the SE model, the CVC must be able to operate with a static capacitance of (4±2) pF with a detectable capacitance variation of ±2 pF, the range of conversion factors is 0.5 to 0.95 V/pF. The characteristics of CVC heavily depend on the operational amplifier's performance. For the 400 kHz clock frequency case, the amplifier gain-bandwidth product must exceed 2 MHz [16, 17]. The DC gain must exceed 80 dB. The required signal-to-noise ratio and non-linear distortion must be at least 80 dB.

Based on these requirements, we designed a fully-differential folded cascode operational amplifier with a complementary input pair and a class AB output stage. Complementary pair at the input of the amplifier allows operation with input voltages that have an amplitude from ground to power supply. The class AB output amplifier stage provides a large current, which in turn allows the operational amplifier to operate with a resistive load or with a large capacitive load. A continuous time common-mode feedback circuit has been implemented to stabilize the amplifier's operating point. The designed amplifier has the following characteristics: DC gain 108 dB, phase margin 64 degrees, 70 MHz gain bandwidth, signal-to-noise and nonlinear distortion ratio 92 dB, current consumption 1.1 mA.

3) Low-pass filter with programmable gain

A low-pass filter (LPF) is required to suppress unwanted signals in the high-frequency band before the signal can be digitized. This is also called an anti-aliasing filter.

CMOS technology utilizes active RC filters or switched-capacitor filters. Switched-capacitor filters have low sensitivity to process variations because the filter characteristics are determined by the ratio of capacitors' values and the characteristics of the operational amplifier. However, the proper operation of such filters requires operational amplifiers with a sufficiently wide bandwidth and high gain. The characteristics of the operational amplifier developed for CVC, meet these requirements. In this regard, LPF is also based on this amplifier. In this paper, a first order filter is used. The bandwidth of the LPF can be adjusted by the control register within 5.4–25 kHz and the gain within 8–32 dB.

4) Analog-to-digital converter

An ADC with at least 13-bit resolution, a conversion rate of 500 ksps and a low phase delay is required for a MMG with these characteristics. Successive-approximation ADC satisfies these requirements. The schematic implementation of the successive-approximation ADC utilizes a differential capacitive digital-to-analog converter. The successive-approximation register is implemented using synchronous digital circuitry.

Nonlinear behavioral model

At this stage, the model takes into account nonlinear dependencies to describe the "gap-closing" electrode structure of the secondary SE axis:

- displacement to capacitance conversion

$$C_1(\alpha) = \frac{\varepsilon_0 S}{d - \alpha R_{cp}}, \tag{4}$$

where α – angular displacement of the moving mass on the secondary axis; S – electrode overlap area; $\varepsilon_0 = 8.854e^{-12}$ F/m – vacuum permittivity; d – electrode spacing;

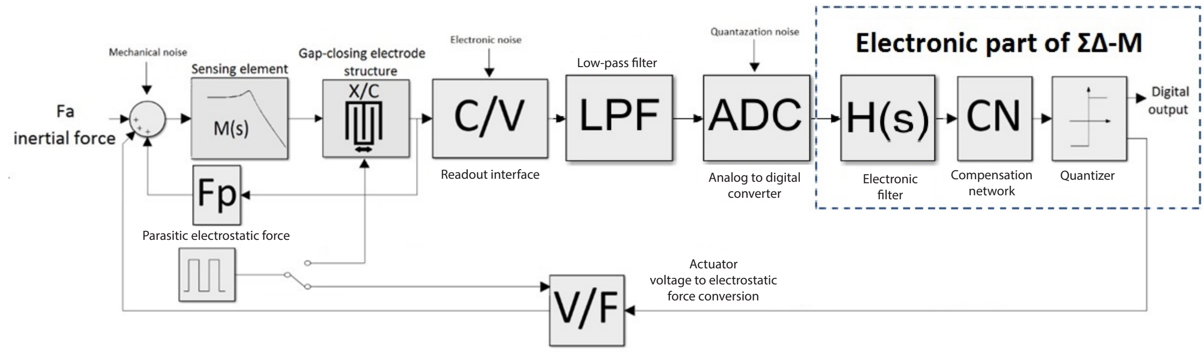

Fig. 5. Nonlinear behavioral model of the secondary oscillation loop

- electrode voltage to electrostatic torque conversion

$$M(\alpha,U) = -\frac{1}{2}\frac{dC}{d\alpha}\cdot U^2 = \frac{1}{2}\frac{\varepsilon_0 S R_{cp}}{\left(d-\alpha R_{cp}\right)^2}\cdot\frac{U^2}{2}, \tag{5}$$

where U – electrode voltage.

In addition, the model is enhanced by a detailed description of the sensing and driving methods. Time division is taken into account (Fig. 5), as well as the parasitic electrostatic moment acting on the sensing electrodes.

Since the sensor operates in the compensation mode in the zero point region, the nonlinear harmonics in the output signal must also tend to zero.

Refined system model with regard to the results of FEM-analysis of SE design

In order to further improve the parameters of the SE, in particular to take into account the full, unsimplified geometry, boundary effects, parasitic effects, technological errors, as well as high-frequency harmonics caused by natural vibrations of the electrodes, we performed a finite-element analysis of the entire structure and its individual elements in the COMSOL Multiphysics [20]. The results were transferred to system model (Fig. 6).

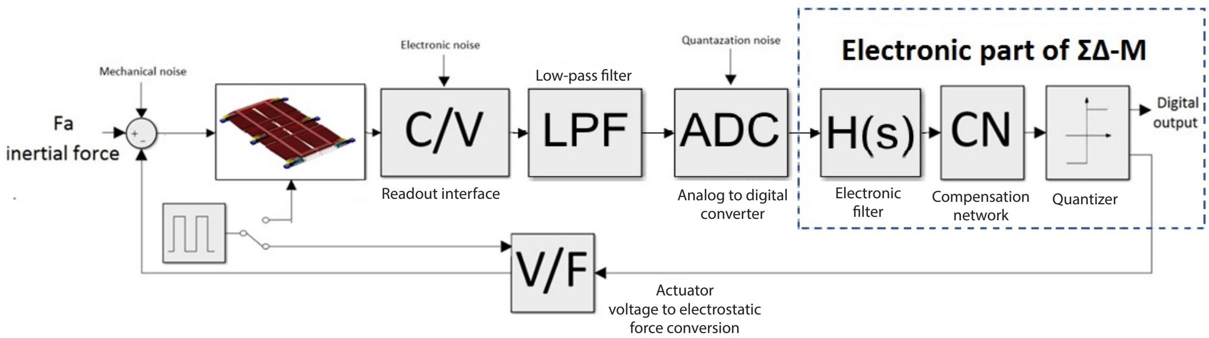

Fig. 6. Refined system model with regard to the results of FEM-analysis of SE design

Simulation results

Fig. 7 and 8 show the spectrum of the output signal of the delta-sigma modulator and its enlarged fragment, showing the area around the frequency of 8 kHz, obtained by simulation of the refined system model in Matlab/Simulink.

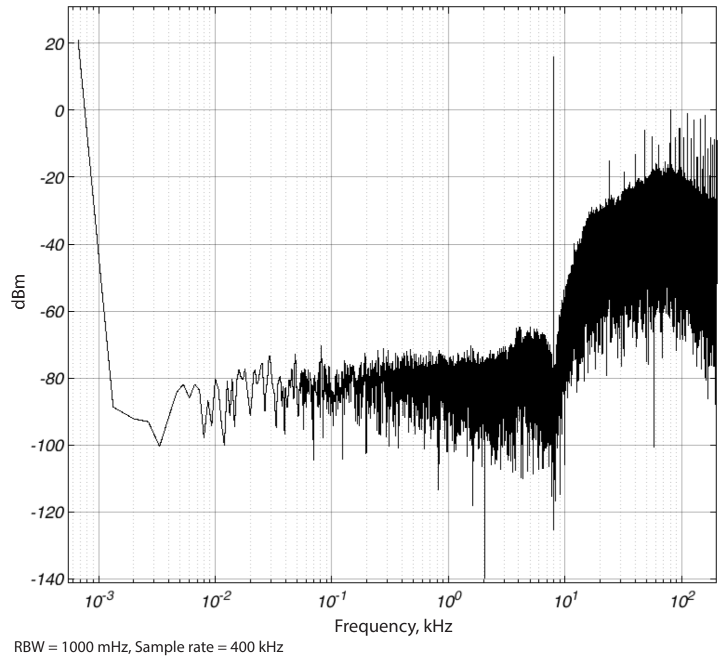

Fig. 7. Output spectrum of delta-sigma force feedback gyroscope including additional effects

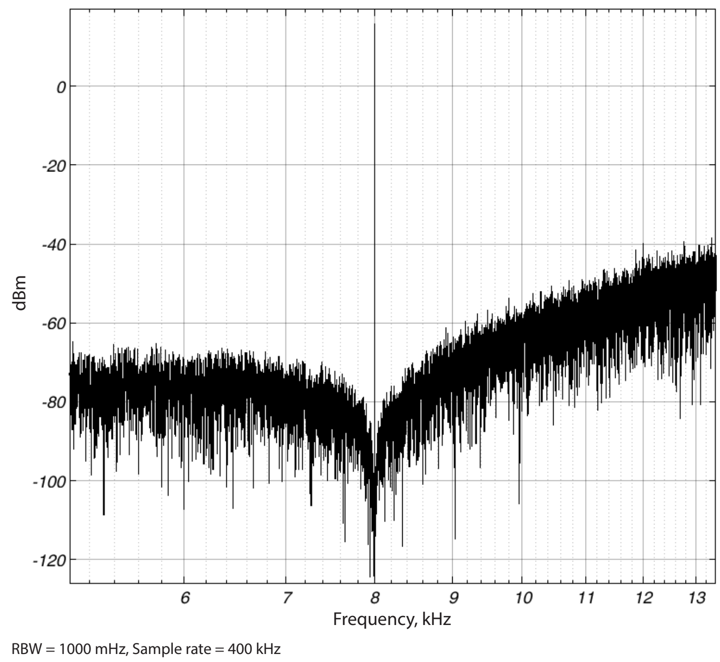

Fig. 8. Enlarged area of the output spectrum around the 8 kHz frequency

The output signal spectrum corresponds to the spectrum of the output signal for the electromechanical delta-sigma modulator with the 8 kHz eigenfrequency of the SE, presented in Fig. 3 and obtained for the refined system model. The spectrum shows nonlinear distortions at multiples of harmonics and the effect of the electronic blocks transfer functions on the noise spectrum. A signal-to-noise ratio of more than 80 dB is achieved for a bandwidth of 100 Hz. Fig. 7 and 8 are obtained at a sampling rate of 400 kHz and a frequency resolution of 1 Hz.

Test results

Fig. 9 shows a block diagram of the corresponding to the testbench. The analog part of the prototype (CVC, LPF and ADC blocks) is implemented in the form of an integrated circuit, manufactured at the X-FAB factory using XH018 technology. Due to the complexity of the control system algorithms and requirement for flexible adjustment of analog and digital blocks, taking into account the parameters of the real SE, the digital part of the processing circuit is implemented using FPGA. Based on the system model, the optimal values of the system parameters were obtained, in particular, the shape of the control pulses, the coefficients of forward and backward connections in the ΣΔ-M, the coefficients of digital filters, the amplification coefficients and the value of phase delay, etc. We used the interface board and LabVIEW software to support data processing and analysis on a personal computer (PC). It is also possible to use the SPI interface to work with the register memory of the IC and the FPGA, to write data from the output of each block and to perform real-time testing and configuration. The output signals of each digital block can be analyzed in time and frequency domain.

As a SE, we employed the RR-type MMG SE developed at Concern CSRI Elektropribor, JSC.

Fig. 10 shows the measured electromechanical ΣΔ-M output signal of force-feedback MMG. The output spectrum shape corresponds with that shown in Fig. 8. For the assembled prototype, the eigenfrequency of the particular gyroscope SE sample is 8.8 kHz. We configured the electronic part of the ΣΔ-M, so that the maximum signal-to-noise ratio is achieved at the specified eigenfrequency of the particular SE. For the implemented prototype, the signal-to-noise ratio was experimentally obtained at 60 dB at the least, which may be due to the inaccuracy of coefficient transfer in digital form, as well as extra unaccounted system parameters when setting the coefficients.

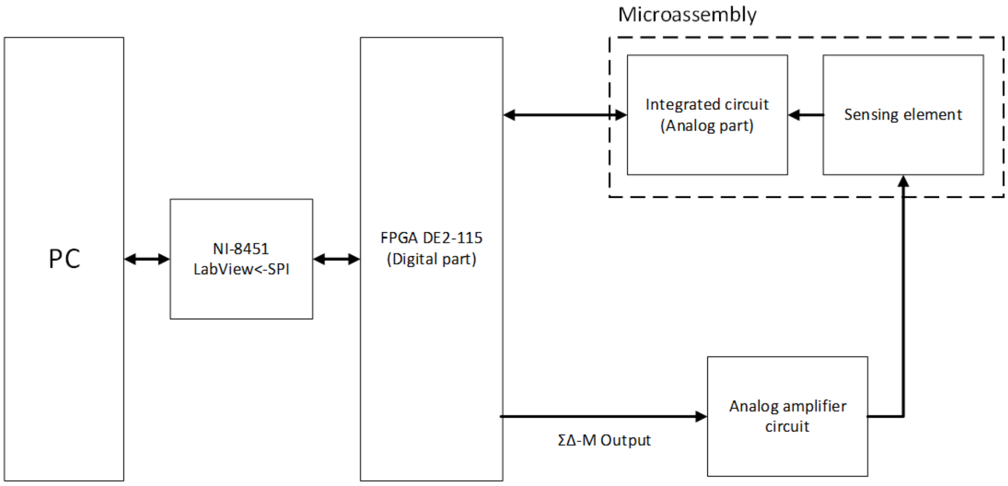

Fig. 9. Testbench block diagram

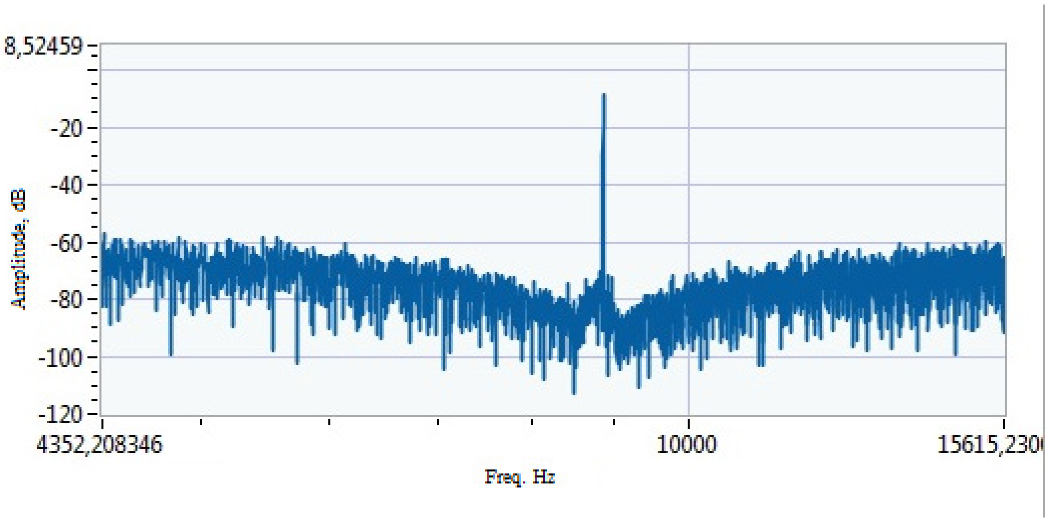

Fig. 10. Spectrum of electromechanical ΣΔ-M output obtained from testbench

Conclusion

The paper proposes a methodology for the design of inertial MEMS based on a system model. We developed a system model taking into account real parameters of SE, such as nonlinear effects and parasitic dependences, feedback structure architecture, parameters of analog and digital processing blocks, as well as experimental data. Designed system model allows to develop requirements for the IC blocks, and to evaluate the performance of individual blocks and the entire gyroscope.

The addition of experimental data, SE and IC parameters of the system model allow the implementation of the digital twin concept to improve design results.

The assembled IC prototype, which includes the analog part, with the digital part on the FPGA allowed us to perform an additional study of MMG and verify the inherent engineering decisions with the minimization of risks in the development of the specialized IC.

Following the results of prototype studies, we introduced the digital part on the FPGA into the specialized IC and launched its manufacturing.

REFERENCES

1. **Peshekhonov V.G.** Perspektivy razvitiya giroskopii [The Outlook for Gyroscopy]. *Giroskopiya i navigatsiya* [*Gyroscopy and Navigation*], 2020, Vol. 28, No. 2 (109), Pp. 3–10. (rus). DOI: 10.17285/0869-7035.0028

2. **Yazdi N., Ayazi F., Najafi K.** Micromachined inertial sensors. *Proceedings of IEEE*, 1998, Vol. 86, No. 8, Pp. 1640–1659.

3. **Geen J., Krakauer D.** New iMEMS® angular-rate-sensing gyroscope. *Analog Dialog*, 2003, Vol. 37, No. 3, Pp. 1–4.

4. **Acar C., Schofield A.R., Trusov A.A., Costlow L.E., Shkel A.M.** Environmentally robust MEMS vibratory gyroscopes for automotive applications. *IEEE Sensors Journal*, 2010, Vol. 9, No. 12, Pp. 1895–1906. DOI: 10.1109/JSEN.2009.2026466

5. **Watson J.** MEMS gyroscope provides precision inertial sensing in harsh, high temperature environments. Available: *https://www.analog.com/media/en/technical-documentation/tech-articles/MEMS-Gyroscope-Provides-Precision-Inertial-Sensing-in-Harsh-High-Temps.pdf* (Accessed: 08.05.2021).

6. **Yoon S.W., Lee S., Najafi K.** Vibration-induced errors in MEMS tuning fork gyroscope. *Sensors and Actuators*, 2012, Vol. 180, Pp. 32–44. DOI: 10.1016/j.sna.2012.04.022

7. **Chen F., Li X., Kraft M.** Electromechanical sigma delta modulators force feedback interfaces for capacitive MEMS inertial sensors: A Review. *IEEE Sensors Journal*, 2016, Vol. 16, No. 17, Pp. 6476–6495. DOI: 10.1109/JSEN.2016.2582198

8. **Chen D., et al.** A straightforward approach for synthesizing electromechanical sigma-delta MEMS accelerometers. *Sensors*, 2020, Vol. 20, No. 1, P. 91.

9. **Gad M., Elshennawy A., Ismail A.** A design method for delta sigma force-feedback accelerometer interface systems. *2020 18th IEEE International New Circuits and Systems Conference* (*NEWCAS*), IEEE, 2020, Pp. 5–8.

10. **Xiong X., Li Z., Han K.** Comparative study of single quantization architecture and dual quantization architecture electromechanical sigma-delta modulators for MEMS accelerometer. *2020 IEEE International Symposium on Inertial Sensors and Systems* (*INERTIAL*), IEEE, 2020, Pp. 1–4.

11. **Chiang C.T.** Design of a CMOS MEMS accelerometer used in IoT devices for seismic detection. *IEEE Journal on Emerging and Selected Topics in Circuits and Systems*, 2018, Vol. 8, No. 3, Pp. 566–577.

12. **Jun J., et al.** An SC interface with programmable-gain embedded delta sigma ADC for monolithic three-axis 3D stacked capacitive MEMS accelerometer. *IEEE Sensors Journal*, 2017, Vol. 17, No. 17, Pp. 5558–5568.

13. **Chen D., et al.** A ΣΔ closed-loop interface for a MEMS accelerometer with digital built-in self-test function. *Micromachines*, 2018, Vol. 9, No. 9, P. 444.

14. **Li X., Hu J., Liu X.** A high-performance digital interface circuit for a high-Q micro-electromechanical system accelerometer. *Micromachines*, 2018, Vol. 9, No. 12, P. 675.

15. **Lima V., et al.** Small-size MEMS accelerometer encapsulated in vacuum using sigma-delta modulation. *2020 IEEE International Symposium on Inertial Sensors and Systems* (*INERTIAL*), IEEE, 2020, Pp. 1–4.

16. **Bafandeh A., Yavari M.** Digital calibration of amplifier finite DC gain and gain bandwidth in MASH ΣΔ modulators. *IEEE Transactions on Circuits and Systems II*: *Express Briefs*, 2015, Vol. 63, No. 4, Pp. 321–325.

17. **Hussain A., Hanif M.** Active-pasisve delta-sigma modulator ADC for MEMS accelecrometers. *2017 International Symposium on Recent Advances in Electrical Engineering* (*RAEE*), IEEE, 2017, Pp. 1–5.

18. **Lukin A.V., Popov I.A., Belyayev Ya.V., Styazhkina A.V.** Nelineynaya dinamika mikromekhanicheskogo giroskopa RR-tipa v usloviyakh vibratsionnykh vozdeystviy [Nonlinear dynamics of an RR-type micromechanical gyroscope under vibration conditions]. *Materialy XXII konferentsii molodykh uchenykh s mezhdunarodnym uchastiyem: Navigatsiya i upravleniye dvizheniyem* [*Proceeding of the XXII Conference on Navigation and Motion Control*], St. Petersburg, 2020, Pp. 37–40. (rus)

19. **Belyaev Ya.V., Belogurov A.A., Kostygov D.V., Lemko I.V., Mihteeva A.A., Yakimova A.V., Nevirkovets N.N., Chernetskaya N.M.** Design of a micromechanical accelerometer. *25th Saint Petersburg International Conference on Integrated Navigation Systems*, St. Petersburg, 2018.

20. **Yakimova A.V., Belogurov A.A., Belyaev Y.V.** Design of sensing element of micromachined capacitive MEMS accelerometer. *Proceeding of the XIX Conference on Navigation and Motion Control*, St. Petersburg, 2017, Pp. 92–97.

21. **Smirnov I.S., Belyayev Ya.V., Nevirkovets N.N.** Deterministic algorithm for designing an operational amplifier for an accelerometer integrated circuit. *Proceeding of the XXI Conference on Navigation and Motion Control*, St. Petersburg, 2019, Pp. 201–203. (rus)

Received 26.05.2021.

СПИСОК ЛИТЕРАТУРЫ

1. **Пешехонов В.Г.** Перспективы развития гироскопии // Гироскопия и навигация, 2020. Т. 28. № 2 (109). С. 3–10. DOI: 10.17285/0869-7035.0028

2. **Yazdi N., Ayazi F., Najafi K.** Micromachined Inertial Sensors // Proc. of IEEE.-1998. Vol. 86. No. 8. Pp. 1640–1659.

3. **Geen J., Krakauer D.** New iMEMS® angular-rate-sensing gyroscope // Analog Dialog. 2003. Vol. 37. No. 3. Pp. 1–4.

4. **Acar C., Schofield A.R., Trusov A.A., Costlow L.E., Shkel A.M.** Environmentally robust MEMS vibratory gyroscopes for automotive applications // IEEE Sensors Journal. 2010. Vol. 9. No. 12. Pp. 1895–1906. DOI: 10.1109/JSEN.2009.2026466

5. **Watson J.** MEMS gyroscope provides precision inertial sensing in harsh, high temperature environments // URL: https://www.analog.com/media/en/technical-documentation/tech-articles/MEMS-Gyroscope-Provides-Precision-Inertial-Sensing-in-Harsh-High-Temps.pdf (Дата обращения: 08.05.2021).

6. **Yoon S.W., Lee S., Najafi K.** Vibration-induced errors in MEMS tuning fork gyroscope // Sensors and Actuators. 2012. Vol. 180. Pp. 32–44. DOI: 10.1016/j.sna.2012.04.022

7. **Chen F., Li X., Kraft M.** Electromechanical sigma delta modulators force feedback interfaces for capacitive MEMS inertial sensors: A Review // IEEE Sensors Journal. 2016. Vol. 16. No. 17. Pp. 6476–6495. DOI: 10.1109/JSEN.2016.2582198

8. **Chen D., et al.** A straightforward approach for synthesizing electromechanical sigma-delta MEMS accelerometers // Sensors. 2020. Vol. 20. No. 1. P. 91.

9. **Gad M., Elshennawy A., Ismail A.** A design method for delta sigma force-feedback accelerometer interface systems // 2020 18th IEEE Internat. New Circuits and Systems Conf. IEEE, 2020. Pp. 5–8.

10. **Xiong X., Li Z., Han K.** Comparative study of single quantization architecture and dual quantization architecture electromechanical sigma-delta modulators for MEMS accelerometer // 2020 IEEE Internat. Symp. on Inertial Sensors and Systems. IEEE, 2020. Pp. 1–4.

11. **Chiang C.T.** Design of a CMOS MEMS accelerometer used in IoT devices for seismic detection // IEEE Journal on Emerging and Selected Topics in Circuits and Systems. 2018. Vol. 8. No. 3. Pp. 566–577.

12. **Jun J., et al.** An SC interface with programmable-gain embedded delta sigma ADC for monolithic three-axis 3D stacked capacitive MEMS accelerometer // IEEE Sensors Journal. 2017. Vol. 17. No. 17. Pp. 5558–5568.

13. **Chen D., et al.** A ΣΔ closed-loop interface for a MEMS accelerometer with digital built-in self-test function // Micromachines. 2018. Vol. 9. No. 9. P. 444.

14. **Li X., Hu J., Liu X.** A high-performance digital interface circuit for a high-Q micro-electromechanical system accelerometer // Micromachines. 2018. Vol. 9. No. 12. P. 675.

15. **Lima V., et al.** Small-size MEMS accelerometer encapsulated in vacuum using sigma-delta modulation // 2020 IEEE Internat. Symp. on Inertial Sensors and Systems. IEEE, 2020. Pp. 1–4.

16. **Bafandeh A., Yavari M.** Digital calibration of amplifier finite DC gain and gain bandwidth in MASH ΣΔ modulators // IEEE Transactions on Circuits and Systems II: Express Briefs. 2015. Vol. 63. No. 4. Pp. 321–325.

17. **Hussain A., Hanif M.** Active-pasisve delta-sigma modulator ADC for MEMS accelecrometers // 2017 Internat. Symp. on Recent Advances in Electrical Engineering. IEEE, 2017. Pp. 1–5.

18. **Лукин А.В., Попов И.А., Беляев Я.В., Стяжкина А.В.** Нелинейная динамика микромеханического гироскопа RR-типа в условиях вибрационных воздействий // Матер. XXII конф. молодых ученых с международным участием: Навигация и управление движением. 2020. С. 37–40.

19. **Belyaev Ya.V., Belogurov A.A., Kostygov D.V., Lemko I.V., Mihteeva A.A., Yakimova A.V., Nevirkovets N.N., Chernetskaya N.M.** Design of a micromechanical accelerometer // 25th Saint Petersburg Internat. Conf. on Integrated Navigation Systems. St. Petersburg, 2018.

20. **Yakimova A.V., Belogurov A.A., Belyaev Y.V.** Design of sensing element of micromachined capacitive MEMS accelerometer // Proc. of the XIX Conf. on Navigation and Motion Control, St. Petersburg, 2017. Pp. 92–97.

21. **Смирнов И.С., Беляев Я.В., Невирковец Н.Н.** Детерминированный алгоритм проектирования операционного усилителя для интегральной схемы акселерометра // Матер. XXI конф. молодых ученых с международным участием: Навигация и управление движением. 2019. С. 201–203.

Статья поступила в редакцию 26.05.2021.

THE AUTHORS / СВЕДЕНИЯ ОБ АВТОРАХ

Tulaev Artyom T.
Тулаев Артём Толибович
E-mail: artulaev@gmail.com

Styazhkina Anna V.
Стяжкина Анна Васильевна
E-mail: anna_yakimov@mail.ru

Kozlov Alexey S.
Козлов Алексей Сергеевич
E-mail: kas573@yandex.ru

Belyaev Yakov V.
Беляев Яков Валерьевич
E-mail: jak0b@mail.ru